AKADÉMIAI KIADÓ

UNIVERSITY of DEBRECEN

International Review of Applied Sciences and Engineering

13 (2022) 2, 228–238

DOI:
10.1556/1848.2021.00354

ORIGINAL RESEARCH PAPER

Delamination buckling of a laminated composite shell panel using cohesive zone modelling

Ikram Feddal* and Abdelatif Khamlichi

Department of Industrial and Civil Sciences and Technologies, National School of Applied Sciences, University Abdelmalek Essaadi, 93030, Tetouan, Morocco

Received: July 30, 2021 • Accepted: October 7, 2021
Published online: December 16, 2021

ABSTRACT

Laminated composite shell panels take part in several engineering structures. Due to their complex nature, failure modes in composites are highly dependent on the geometry, direction of loading and orientation of the fibers. However, the design of composite parts is still a delicate task because of these fiber failure modes, which includes matrix failure modes or other so-called interlaminar interface failure such as delamination, that corresponds to the separation of adjacent layers of the laminate as a consequence of the weakening of interface layer between them. In this work, impact-induced delamination represented as a circular single delamination is investigated, as it can reduce greatly the structural integrity without getting detected. Furthermore, attention is focused on its effect upon the post-buckling response and the compressive strength of a composite panel. The delamination buckling was modelled using the cohesive element technique under Abaqus software, in order to predict delamination growth and damage propagation while observing their effects on the critical buckling load.

KEYWORDS

composite panel, buckling, delamination, cohesive elements, finite element method

1. INTRODUCTION

Aerospace industry are increasingly moving towards the massive use of composite materials in aircraft structures such as in Airbus 350, Airbus 380 and Boeing 787 [1]. Composites have attractive mechanical properties like the increased strength and high specific stiffness combined with weight reduction, compared to conventional materials. Hence, the extensive use of composite materials instead of aluminum alloys, contributes to reduce operating costs significantly. This makes it possible to meet the prediction announced in the aeronautics industry to reduce costs by 20% over the short period and to consider a 50% reduction in the long term [2]. These advantages should not cover fragility of composites to undergo damage even under low-speed impacts. This is due to the low thicknesses used and the risk of inter-ply delamination which corresponds to the decohesion of two layers of the laminate. This damage can be caused by falling tools during manufacturing and maintenance operations, bird strike, and can seriously degrade the laminate's compressive strength and buckling stability [3, 4].

Due to their complex nature, failure modes in composites are highly dependent on the geometry, direction of loading and orientation of the plies [5]. There is damage at the level of the fibers, at the level of the matrix or other so-called inter-laminar as delamination, which is a particular concern. It is one of the predominant forms of damage caused by manufacturing defects and high stress concentrations due to geometric discontinuity [6]. In buckling conditions, delamination can expand and further reduce the strength of composite structures. It then poses a serious threat to the safety of the structure and the consequences can be catastrophic.

Delamination is a failure in a composite material, which leads to the separation of plies. It is due to various causes such as [7]:

*Corresponding author.
E-mail: ikramfeddal@gmail.com

AKJournals

- Geometric discontinuities: Stresses that occur between stiffeners and thin plates, free edges, joints, and holes promote the initiation of delamination and trigger mechanisms of delamination between plies. In a laminate composed of several plies with various orientations, the plies mutually limit the deformations of Poisson by developing interline shear stresses, also as normal stresses, counting on the direction of the thickness. A transfer of interlaminar loads occurs particularly at the sides of the structure and may cause delamination.
- Curved sections: In the case of curved segments, tubes, cylinders and spheres under pressure, normal and shear stresses develop at the interface of two adjacent layers. they'll cause an interlaminar crack to develop and cause loss of adhesion.
- Hygrothermal effects: The difference within the thermal expansion coefficients of the matrix and therefore the reinforcement leads to mechanical stresses under thermal gradients which may be a source of delamination also as mechanical changes. Furthermore, the anisotropic dimensional response of the laminates because of moisture absorption can also cause interline cracks. Plasticization of the polymer matrix and chemical deterioration of the constituent materials due to interaction with penetrating water may end in additional damage like cracks or cracks within the matrix.
- Poor manufacturing process: Delamination can arise from the manufacturing stage on account of non-uniform resin distribution or because of the presence of voids resulting from improper practices when applying the layers. Residual stresses also can be induced by differential shrinkage of the constituents upon cooling from the cure temperature to ambient temperature.
- Low speed impacts: Transverse concentrated loads caused by low-energy impacts, like a tool dropped during maintenance or propelled runway debris during take-off or landing, may cause interlaminar detachment between adjacent plies having different orientations. Impact-induced delamination is initiated because of the interaction of the matrix cracks and therefore the resin-rich zone along the ply interface. This is often likely to end in complex damage with multiple delamination, fiber rupture and matrix cracks. These damages are classified as BVID (Barely Visible Impact Damage), they arise below the surface of the laminate and are not easily detected during maintenance tasks. This explains why impact damage is so of concern when designing a composite structure, because undetected hidden delamination can cause ruptures with none external warning signs [8].

Juhász and Szekrényes [9] have studied the effect of delamination on the critical buckling force of composite plates where orthotropic rectangular plates with through-the-width delamination are modelled using special sorts of Mindlin plate finite elements. It had been found that the presence of delamination with different sizes is affecting the buckling loads. Also, for the generalization of the results, they have used an equivalent boundary conditions and layup with different plate sizes, only the ratio of the delamination and also the plate length matters.

Chen et al. [10] have developed an analytical model with a generalized Rayleigh–Ritz approach so as to review the characteristics of the buckling response of VAT (Variable angle tow) composite plates with the width, or an embedded rectangular delamination under axial compressive loading. Numerical results of VAT composite plates with one delamination were obtained with reference to various delamination sizes and positions. It had been found that the in-plane deformation of delaminated portions within the delamination region is vitally important for the delamination buckling analysis. The buckling loads decrease with a rise in delamination size.

Monda and Ramachandra [11] have investigated numerically the nonlinear dynamic pulse buckling of imperfect composite plate with embedded delamination, the dynamic buckling load is calculated using Tsai-Wu quadratic interaction criterion. The results have showed that the varied sort of impulsive loading, plate condition affects the pulse global buckling load of the structure. Moreover, the delamination may arise reducing the stiffness of the plate which results in the buckling of the structure then its collapse.

The shape of the various delamination resulting from an impact is complex and depends on the geometry of the structure, the properties of the fabric and therefore the impact energy. The active damage mechanisms are more complex than within the case of simple delamination, but the geometry observed during experimental tests is often incorporated or simplified during finite element simulation. The delamination zone is often taken as a square, circular or elliptical domain so as to confirm a satisfactory compromise between the important realistic representation of the geometry of the real delamination and also the simple insertion of the artificial damage. The placement of non-adhesive inserts of known shape and position in the structures allows the effect of delamination geometry on mechanical properties to be studied in a more controlled manner. In the study presented in this paper, we have considered only the case of damage induced by an impact and represented by a circular delamination.

2. DELAMINATION BUCKLING

Delamination may result during a significant reduction within the compressive strength of a carbon fiber reinforced polymer (CFRP) composite structure. A drastic reduction in bending stiffness is additionally observed. In the presence of compressive loads [12], interline cracks can trigger the local buckling of the thinnest sub-laminate. Once buckling occurs, interline delamination can expand and further reduce the strength of the structure. Fuselage panels and upper wing skins are samples of composite components that are particularly sensitive to in-service compression buckling and shear loads [13]. Due to the complexity of the analysis of those structures, which response is extremely nonlinear,

engineers are reluctant to explore all the alternatives offered and thus limit the chances of design optimization. Especially, analysis within the field of post-buckling, during which nonlinearities play a dominant role, is extremely laborious [14]. What characterizes delamination buckling is the complex interaction between integrated delamination and therefore the response to buckling and post-buckling. This results in the reduction in compressive strength as has been demonstrated experimentally in damaged laminates. Therefore, the stresses in these layers are greater than those that would exist in an undamaged panel, which greatly reduces the breaking load [13].

When a delaminated composite panel is subjected to uniaxial compression within the plane, different buckling modes may develop counting on the dimensions and position of delamination. These modes are illustrated within Fig. 1.

Local buckling, as shown in Fig. 1(a), may occur for instance, when the upper sub-laminate is thin and therefore the delaminated area is large. In this case, the stiffness of the upper sub-laminate is low compared to that of the lower sub-laminate and, therefore, it undergoes buckling. the appliance of a further load increment to the local buckling load may trigger a mode change to the mixed buckling mode as shown in Fig. 1(b). This mode may be a combination of local and global buckling modes and should occur before the critical load.

Depending on the case, the overall instability of the structure also can be observed consistent with the overall buckling mode, Fig. 1(c). This mode is characterized by the two layers buckling within the same direction and with an equivalent out-of-plane movement. It is going to be the primary to occur when the initial delamination features a small area and is found near the median surface of the panel.

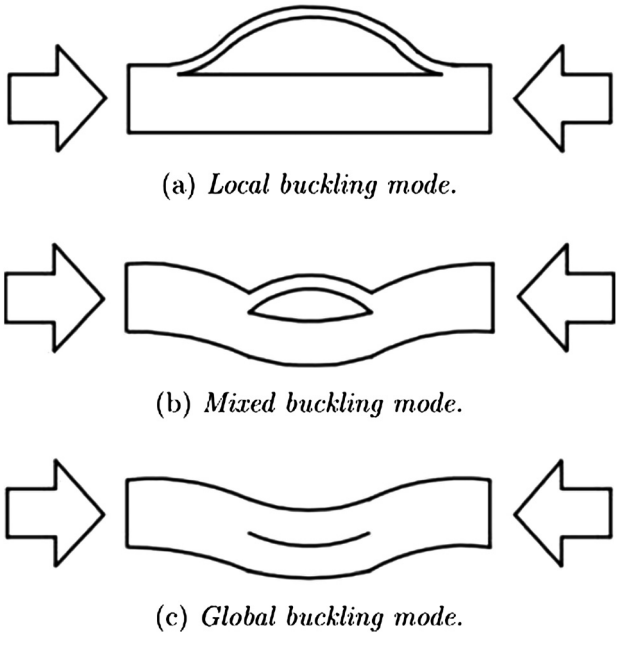

Fig. 1. Buckling modes of a delaminated composite panel

In some cases, the failure load is often reached without spreading the built-in damage.

2.1. Numerical model of delamination: cohesive elements

Several numerical techniques have been proposed to assess the problem of delamination in composite structures. Traditional numerical tools are formulated as part of linear fracture mechanics (LMR). This technique is predicated on Griffith's fracture theory [15] which, consistent with the first law of thermodynamics, postulates that the reduction in strain energy because of crack propagation is employed to form new crack surfaces. This hypothesis is valid for brittle materials, during which the dissipation of the energy derived from the plastic deformation, during the rupture, are often neglected.

Since the nonlinear crack-tip processes happen in a very small plastic area, compared to the tiniest characteristic dimension of the structure, the numerical approaches supported the LMR (Linear Mechanics of Rupture) assume that the fracture mechanisms are often associated with the simple propagation of the delamination front. The growth of the discontinuity occurs when a mixture of the components of the rate of energy release G is such that is equal to or greater than a critical value G_C.

Techniques like J-integral, EDT (Energy Derivative Technique), tangent stiffness, or VCCT (Virtual Crack Closure Technique) are employed to calculate the components of the critical rate of energy release G_C using the principles of LMR. A more modern approach to delamination analysis consists of modelling, in which nonlinear crack-tip processes are represented explicitly instead of being considered to be infinitely localized on the discontinuity front [16, 17]. The formation of a cohesive zone on a spread surface of displacement discontinuity characterizes the progressive degradation of stiffness associated with the irreversible damage that occurs between the laminates.

This approach seems to permit an improved description of the physical mechanisms that develop during cracking by delamination and overcoming some important drawbacks related to models supported the LMR. Nevertheless, the hypothesis of the self-similar spread of delamination, namely that the delamination front does not change its shape throughout the loading history, requires prior knowledge of the location of the crack and therefore the direction of propagation. This requirement prevents VCCT from getting used for several categories of delamination problems like delamination caused by low-speed impact, because it cannot accurately predict the onset of damage [18, 19].

The formulation of the cohesive elements is based on the CZM (Cohesive Zone Model) model proposed by Dugdale and Barenblatt [20] to simulate complex fracture mechanisms at the crack front. The main advantage of cohesive zone models is the ability to predict the onset and spread of delamination without first knowing the location and direction of defect propagation. Therefore, unlike VCCT, problems such as the study of the compressive behavior of

composite plates containing several built-in artificial delamination as well as the analysis of fracture of composite joints can be investigated numerically. For this reason, the formulation of the cohesive zone has become a very useful tool in the design of damage tolerant composite structures.

The cohesive zone approach models an extended cohesive zone, or process zone, at interfaces where delamination may occur, in which tractions or cohesive forces resist interfacial separations, often referred to as relative displacements in the literature. Indeed, the cohesive damage zone is the part of the cohesive layer closest to the delamination front in which any irreversible degradation of the properties of the interface takes place, Fig. 2. The elements within this zone are characterized by meeting the specified damage initiation criterion which governs the start of the progressive damage process. Physically, the zone of cohesive damage represents the way in which the rigidity of the material degrades locally due to the combination of the cracks around the crack tip (Fig. 3).

According to Camanho and Davila [21], the cohesive zone approaches can be related to Griffith's fracture theory if the size of the cohesive zone is small compared to the characteristic dimensions of the structure. This condition is met by materials that exhibit near-brittle fracture behavior, such as Polyether-ether-ketone (PEEK) or epoxy-based composites used in aerospace structures. The connection between the two theories can be established by setting the area under the tensile-separation curve equal to the corresponding fracture toughness, regardless of its shape. In case of delamination under single-mode loading, we have:

$$\int_0^{\delta_3^f} \tau_3(\delta_3)d\delta_3 = G_{IC};\ \int_0^{\delta_2^f} \tau_2(\delta_2)d\delta_2 = G_{IIC};\ \int_0^{\delta_1^f} \tau_1(\delta_1)d\delta_1 = G_{IIIC} \quad (1)$$

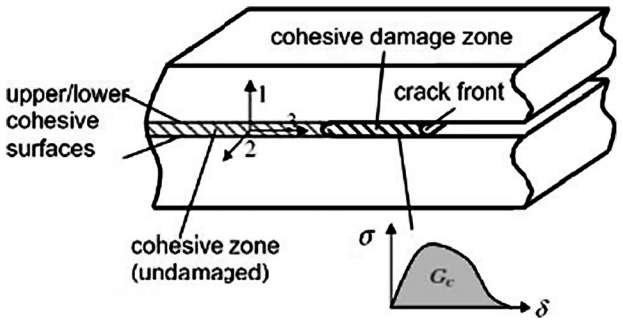

Fig. 2. Cohesive zone model schematic

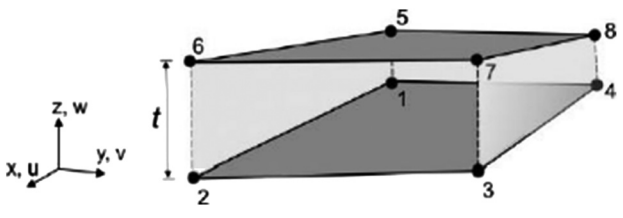

Fig. 3. Geometry of the 8-node cohesive element

Where G_{IC}, G_{IIC} et G_{IIIC} are respectively mode I, mode II and mode III fracture toughness.

δ_3^f, δ_2^f and δ_1^f are the corresponding final separations relative to the crack propagation under single-mode loading.

In general, we can write the expression related to delamination under mixed mode loading as follow:

$$\int_0^{\delta_m^f} \tau_m(\delta_m)d\delta_m = G_C \quad (2)$$

G_C is the mixed-mode fracture toughness
δ_m is the equivalent separation
τ_m is the corresponding equivalent traction
δ_m^f is the final equivalent separation associated to complete debonding.

The so-called zero thickness elements are suitable in situations where the intermediate glue material is extremely thin and for all practical purposes are often considered zero thickness, like the bonded composite laminates investigated during this work. In this case, the macroscopic properties of the fabric are not directly relevant, and that we must use concepts derived from fracture mechanics.

2.2. Constitutive law

The constitutive law which relates the tractions of elements τ to the separations of elements δ expressed in local isoparametric coordinates is:

$$\tau_s = D_{sr}\delta_r \quad (3)$$

The following assumptions are taken into account when defining the constitutive operator D_{sr}:

- Linear elastic response prior to damage onset.

$$\tau_s = K_p\delta_s \quad (4)$$

Where *Kp* is the penalty stiffness.

- Failure of the cohesive element is characterized by progressive degradation of the material stiffness, which is driven by a damage process.
- The cohesive layer does not undergo damage under pure normal compressive stresses or strains.

A single variable constitutive law for delamination in mixed mode is able to follow the evolution of interface damage. The irreversible softening behavior of the cohesive zone and contact problems resulting from compression can be observed by defining the constitutive operator D_{sr} as follows:

$$D_{sr} = \begin{cases} \overline{\delta_{sr}}K_p \\ \overline{\delta_{sr}}K_p\left[(1-d)K_p + dK_p\dfrac{\langle -\delta_3\rangle}{\delta_3}\overline{\delta_{s3}}\right] \\ \overline{\delta_{s3}\delta_{s3}}\dfrac{\langle -\delta_3\rangle}{\delta_3}K_p \end{cases} \quad (5)$$

where $\overline{\delta_{sr}}$ is the Kronecker Delta. Three different areas of material behavior delimited by equivalent separations

corresponding to the appearance of damage δ_m^0 and total decohesion δ_m^f can be identified:

- Linear elastic response before the onset of damage (5.a)
- Gradual softening during additional loading after the onset of damage (5.b)
- Control of the propagation of damage following the ultimate failure of the element (5.c)

It is noted that the constituent equation is coupled with the law of specified damage evolution through the values of critical separations δ_m^0 and δ_m^f, which can be calculated by defining respectively the appropriate criteria for occurrence and propagation of damage, and through the variable of global damage d, which depends on the form of the law of softening as well as on δ_m^0 and δ_m^f themselves. The next part discusses an appropriate damage law defined in terms of equivalent separations δ_m and corresponding equivalent tractions τ_m as well as its effect on the critical buckling load.

A. Damage evolution law:

The law of evolution of the damages to be coupled with the constitutive equation in order to describe the behaviour at fracture of the cohesive layer is defined by:

- A criterion for the appearance of damage: The onset of damage refers to the onset of degradation of the stiffness of the cohesive member [22]. The softening process begins when the stresses and/or strains meet a predefined damage initiation criterion. The corresponding values of equivalent separation and equivalent traction are respectively δ_m^0 and τ_m^0.
- In mixed mode loading, the onset of softening behaviour can occur before any of the tensile components reach their own unique allowable mode, namely interlaminar tensile strength N and interlaminar shear forces S and T. Therefore, the criterion for the occurrence of damage must take into account the interaction between normal loads and shear loads. Hence, the criterion for the appearance of damage must take into account the interaction between normal loads and shear loads. In this work, the quadratic constraint criterion proposed by [23] was used because it has been shown to provide reasonable predictions for composite structures [24]:

$$\left(\frac{\langle\tau_3\rangle}{N}\right)^2+\left(\frac{\tau_2}{S}\right)^2+\left(\frac{\tau_1}{T}\right)^2=1 \tag{6}$$

Among the different ways to measure the mode ratio under the mixed mode loading conditions, the mix mode ratio β has been used. For an opening separation δ_3 greater than zero, β is defined as:

$$\beta=\frac{\delta_{cisaillement}}{\delta_3} \tag{7}$$

Using the quadratic stress criterion, the equivalent mixed-mode separation corresponding to the initiation of damage is given by

$$\delta_m^0=\begin{cases}\delta_3^0\delta_1^0\sqrt{\dfrac{1+\beta^2}{\left(\delta_1^0\right)^2+\left(\beta\delta_3^0\right)^2}} & \delta_3>0 \quad (8a)\\ \delta_{cisaillement}^0 & \delta_3\le 0 \quad (8b)\end{cases}$$

Using the same penalty stiffness for modes I, II and III and assuming isotropic shear behaviour, i.e., $S = T$, equivalent separations δ_3^0 , δ_1^0 and $\delta_{cisaillement}^0$ corresponding to the onset of softening under single-mode loading are equal to:

$$\delta_3^0=\frac{N}{K_p},\ \delta_1^0=\delta_2^0=\delta_{cisaillement}^0=\frac{S}{K_p} \tag{9}$$

Finally, the equivalent traction τ_m^0 corresponding to the damage initiation can be calculated as follows:

$$\tau_m^0=K_p\delta_m^0 \tag{10}$$

B. Softening law:

The formulation of the cohesive finite elements is predicated on the CZM approach with the bilinear traction-separation law. Their shape and corresponding parameters are usually determined empirically according to the expected behaviour of the adhesive. Indeed, it is widespread to use a bilinear softening (i.e. triangular) law shape for brittle adhesive and an elasto-plastic (i.e. trapezoidal) shape for ductile adhesive. Among the numerous softening models commonly used (bilinear, exponential, perfectly plastic), the bilinear law is utilized to simulate the various interlaminar toughness tests was adopted within the present study, Fig. 4.

The line AB represents the linear softening envelope of the bilinear constitutive equation. It is assumed that unloading after the appearance of damage occurs linearly towards the origin of tension-separation plane. Reloading after unloading is additionnally performed along an equivalent linear path until the softening envelope is reached. A further reload follows this envelope as indicated by the arrow until it is reached.

Assuming a linear softening law, the global damage variable d is reduced to the expression proposed by Camanho [21]:

$$d=\frac{\delta_m^f\left(\delta_m^{max_m^0}()\right)}{\delta_m^{max_{mm}^{f0}}},\ d\in[0,\ 1] \tag{11}$$

C. Damage propagation criteria:

The definition of an appropriate criterion of propagation of the damages makes it possible to determine the equivalent separation δ_m corresponding to the reduction to zero of the tractions which hold together the faces of the cohesive element. According to the principles of linear elastic fracture mechanics, the growth of mixed-mode delamination is predicted when $G_T \ge G_C$.

Several laws have been implemented in finite element codes to account for the mixing of modes when calculating the toughness of a material, such as the power law's criterion [25], the B-K's criterion [26] and the Reeder's criterion. Indeed, the predictions provided by the B-K criterion are

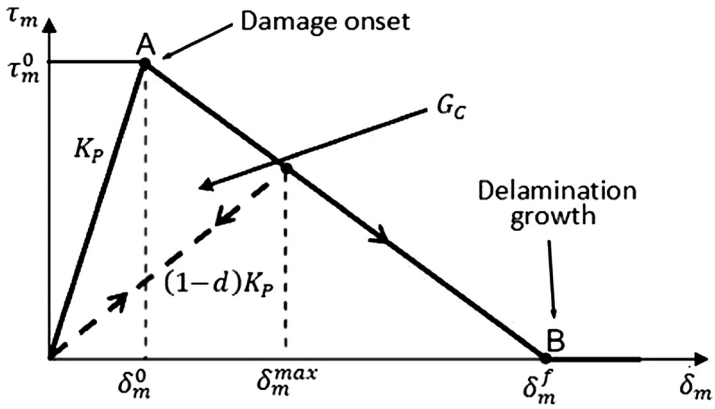

Fig. 4. Linear damage evolution

well in line with the experimental results, as this criterion makes it possible to predict the toughness in mixed mode of materials with the same critical breaking energies for both shear modes. For the linear softening law, the explicit B-K criterion in terms of the mixture ratio of modes is given by:

$$G_{IC} + (G_{IIC} - G_{IC})\left(\frac{\beta^2}{1+\beta^2}\right)^{\eta} = G_C \qquad (12)$$

The parameter η is found by the least squares fitting of the experimental data obtained from a mixed-mode bending test performed at different mode ratios.

3. FINITE ELEMENT MODELLING OF THE DELAMINATION BUCKLING OF A COMPOSITE PANEL

In this work, we will discuss finite element modeling of delamination buckling of composite panels using Abaqus software. A 3D model with an 8-node composite shell member is used. The panel is divided into two sub-laminates by a plane containing the delamination. The two sublayers are modeled separately using an 8-node composite shell member. Appropriate stress conditions are added for the nodes in the safe region. A set of finite element models has been implemented in Abaqus to predict delamination growth and damage evolution while observing their effects on critical buckling load.

The delamination analysis was performed by finite elements using Abaqus software (version 6.19). There are several ways to model the panel for delamination analysis. For the present study, the technique of cohesive elements was adopted. The panel is divided into two regions, the first is the intact region and the other is the cohesive region.

The reduced integration 4 node S4R shell element was used. The reference surface of the sub-laminates was moved from the median surface by using the option OFFSET of the menu of the properties of the shells that makes it possible to model the cohesive contact.

Two levels of mesh refinement were considered in the panel, as shown in Fig. 5.

- Intact region: where the propagation of delamination is not expected. The upper and lower layers of the shell elements are linked together by beam-type multipoint stresses making it possible to simulate the contact connection.
- Cohesive zone: where the propagation of delamination can occur. A layer of cohesive elements was placed between the top and bottom of the shell elements to simulate the evolution of damage in the interlaminar interface.

The solution obtained by using cohesive elements in the simulation of delamination mechanisms is highly dependent on the refinement of the mesh in the cohesive zone region. Indeed, the size of the element in this boundary area determines how the delamination front can extend. In addition, in order to provide realistic predictions of the evolution

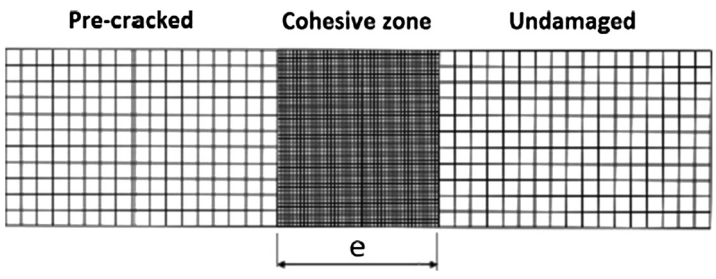

Fig. 5. Mesh patterns of the studied panel

of delamination, the discretization of the cohesive zone must be fine enough to ensure an accurate representation of the interlaminar stress field in front of the crack tip. For these reasons, research on the dependence of the simulated response to the density of the mesh is necessary to select the characteristic size of the cohesive elements (Fig. 6).

A square panel 100 mm ×100 mm with a central circular delamination is considered. The delamination radius R is 40 mm as shown in Fig. 7. Due to panel symmetry, only a quarter of the panel is modeled for finite element analysis.

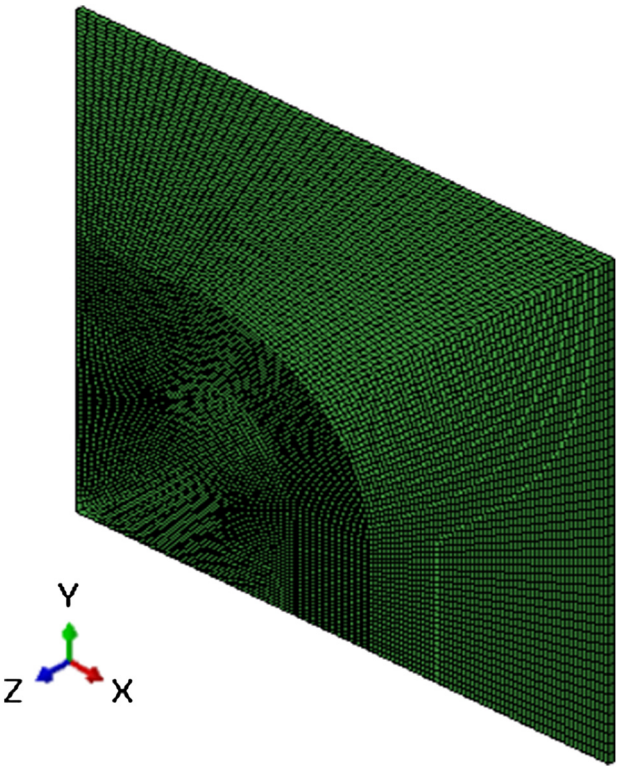

Fig. 6. Finite element model of the considered panel

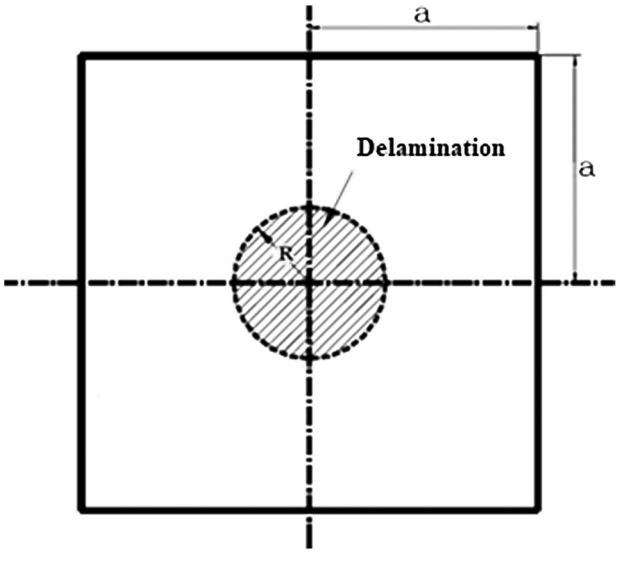

Fig. 7. Geometry of the studied panel

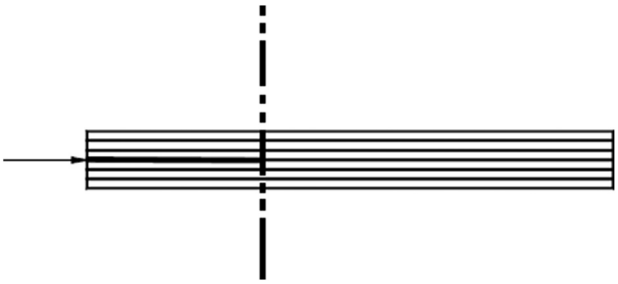

Fig. 8. Position of delamination through the thickness in the composite panel

The position of the delamination through the thickness is considered at the midplane of the laminate (Fig. 8).

```
** MATERIALS
**
*Material, name=Cohesive_material
*Damage Initiation, criterion=QUADS
60., 79.289, 79.289
*Damage Evolution, type=ENERGY, mixed mode behavior=BK, power=2.
 0.9,2.,2.
    *Elastic, type=TRACTION
    100000.,100000.,100000.
*Material, name=carbon_fiber
    *Elastic, type=LAMINA
     57280.7, 57280.7,  0.0452, 4205.64, 4205.64, 4205.64
```

The material used for the numerical simulations is a carbon fiber reinforced Epoxy prepreg composite with a 45-degree ply orientation and, is provided by ILSB (Institute of Lightweight Design and Structural Biomechanics (E317)) [27], E is the Young's modulus, G is the shear modulus,

$$E_1 = E_2 = 57280.65\,MPa,\ \nu_{12} = 0.0452 \text{ and } G_{12} = G_{13} = G_{23} = 4205.64\,MPa$$

As well as the material for the cohesive zone as indicated in the subroutine presented above. The load and boundary conditions corresponding to the uniaxial loading as shown in Fig. 9. We design by u the displacements and θ the rotations.

The aim of this study is to see the effect of behavioral parameters of cohesive elements on the ultimate buckling load in the presence of delamination. For this reason, we have varied a number of parameters such as the Damage initiation criteria and the Quads damage propagation criteria. For each criterion, we took three levels as shown in Table 1.

4. RESULTS AND DISCUSSION

In order to perform a full analysis of the structure, a first linear analysis is considered to determine the Eulerian buckling modes, Fig. 10. Subsequently, a nonlinear analysis of the structure is performed using the Riks algorithm. Initial geometric imperfections can also be introduced into the model.

The analysis makes it possible to deduce the critical buckling load for a perfect composite plate, i.e. delaminated but without having considered initial geometric imperfections, but also for a real plate suffering from imperfections.

Three levels of imperfections were considered: 10%, 20% and 30%, all modal according to the first Eulerian buckling

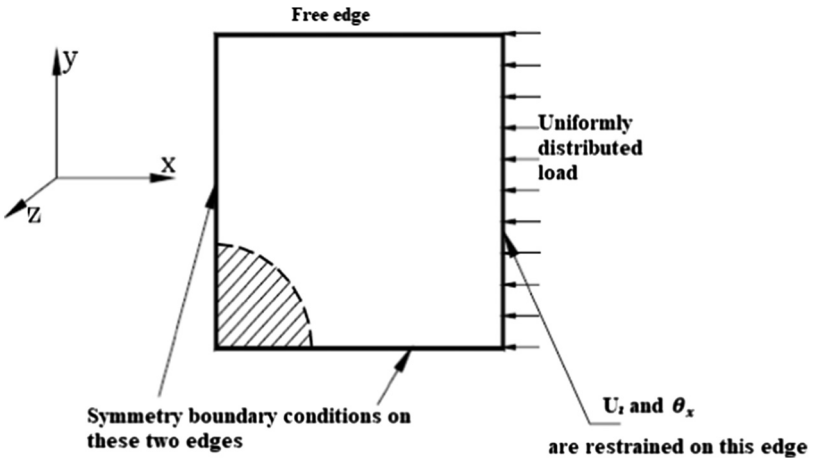

Fig. 9. Boundary conditions and loads

mode of the delaminated composite plate. By recording the value of the limit load, the results obtained are shown in Table 2. This table shows that the critical buckling load decreases as a function of the magnitude of the initial geometric imperfection, which is quite expected. Figure 11 shows an example of the evolution of the curve giving the load as a function of the shortening for the three levels of initial geometric imperfection which were considered.

In order to examine the influence of the cohesive behavior on the buckling resistance, we performed a parametric study in which we varied the damage criteria defined in Table 1 according to a full factorial design containing $3^2 = 9$ combinations. For each case, we calculated the buckling load in the presence of delamination. The results obtained are given in Table 3.

Table 1. Levels of the considered criteria

Initiation damage criteria	Propagation damage criteria
0.9	0.9
1	1
1.1	1.1

Table 2. Levels of the considered criteria

Imperfection's level	Buckling load (N)
10%	11,553
20%	11,136
30%	10,699

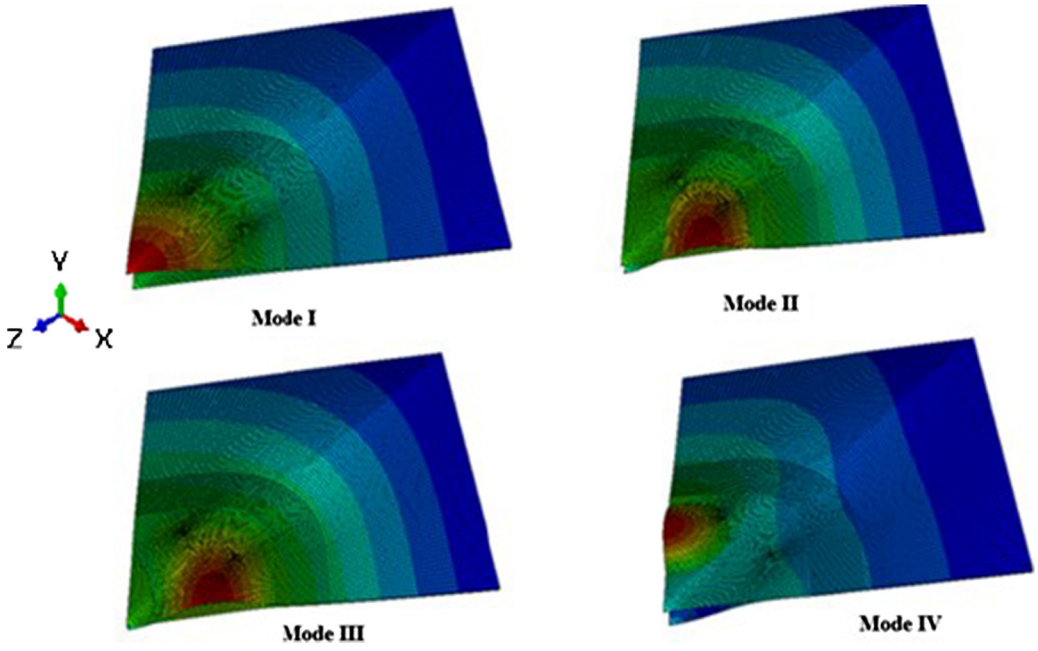

Fig. 10. The first four buckling modes of the composite panel in the presence of a delamination defect

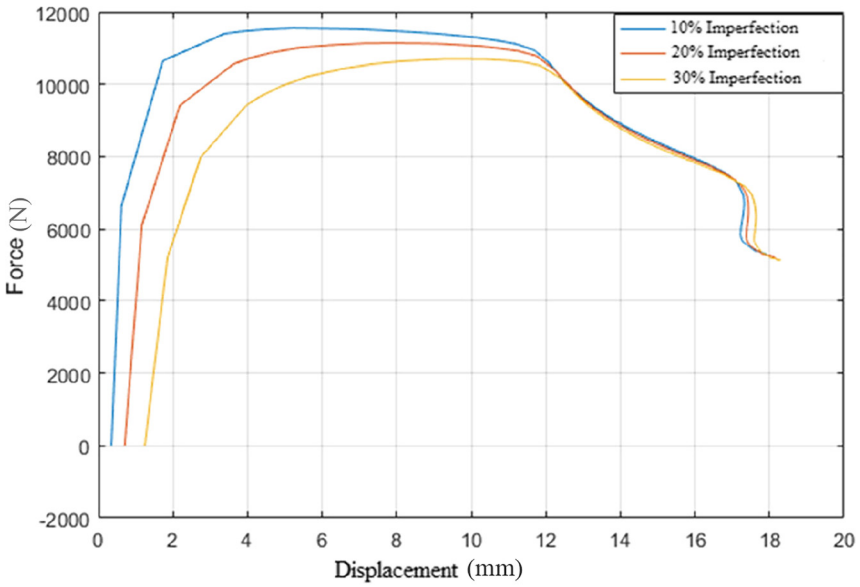

Fig. 11. Force - displacement curve for a composite plate for three different levels of initial imperfection

Table 3. Delamination buckling simulation results

Quads Damage Criterion (Qdc)	Damage Evolution (De)	Buckling load (N)
0.9	0.9	43,165
0.9	1	45,109
0.9	1.1	50,184
1	0.9	47,099
1	1	48,554
1	1.1	54,396
1.1	0.9	47,795
1.1	1	57,449
1.1	1.1	58,498

From Table 3, we can notice that the critical load varies with the two criteria that control the behaviour of cohesive elements. As expected, the critical load increases with the damage initiation threshold and the stiffness of damage propagation. Figure 12 shows the delamination buckling of the composite plate where the onset of delamination growth occurs at a slightly lower load than that associated with the overall buckling. The failure of the delaminated plate occurs during the propagation of the delamination crack.

From Table 3, it is possible to build a polynomial response surface allowing the buckling load to be expressed as a function of the parameters of the cohesive behavior.

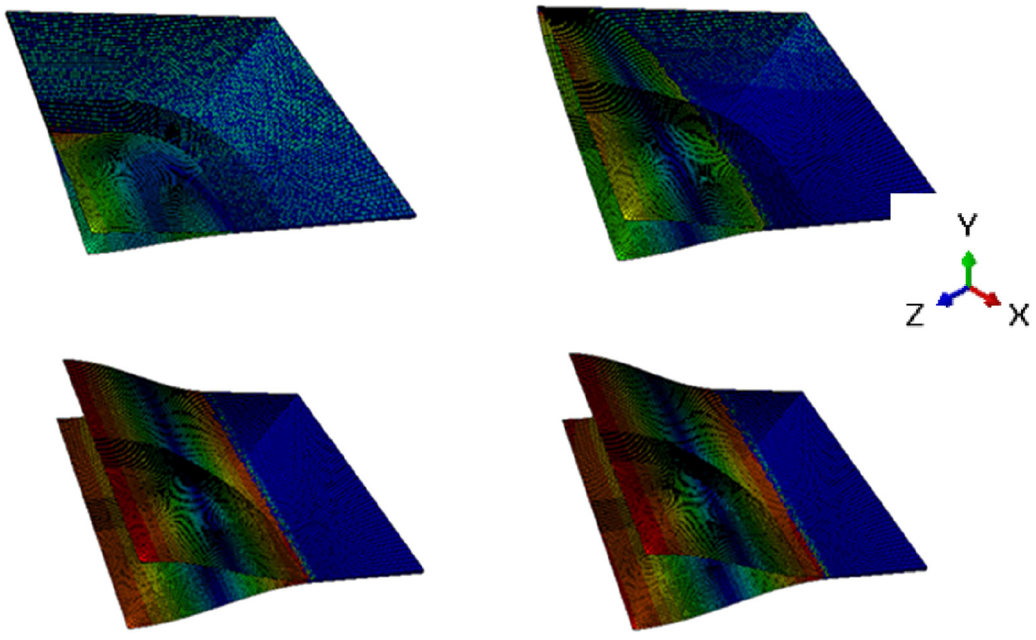

Fig. 12. Buckling of the plate in presence of delamination

Firstly, we've performed an analysis of variance on the results obtained. We have started with a linear model (Table 4), we can notice that it is the initiation threshold factor that has the greatest influence on the variability of the buckling resistance.

The linear model obtained by the "regstats" command of Matlab is written in the form:

$$P_{cr} = 10^4 \times (-0.35905 + 4.21408 \times Qdc + 4.16995 \times De) \quad (13)$$

$$R^2 = 90.7\%$$

We can also derive with an interacting model to improve the representation of the buckling load and increase the coefficient of determination R^2. The results of the analysis of variance are given in Table 5.

The obtained interacting model is given by:

$$P_{cr} = 10^4 \times (5.85295 - 4.99792 \times Qdc - 5.04205 \times De + 9.212 \times Qdc \times De) \quad (14)$$

$$R^2 = 92.15\%$$

Finally, we can interpolate the results obtained using a quadratic polynomial. We then find:

$$P_{cr} = 10^4 \times (7.53268 - 11.9989 \times Qdc - 1.42305 \times De + 9.212 \times Qdc \times De + 3.5005 \times Qdc^2 - 1.8095 \times De^2) \quad (15)$$

$$R^2 = 92.3\%$$

We note that the quadratic model is complex but that it does not provide more information on the correlation than the interacting model. The coefficient of determination R2 does not improve significantly compared to the interacting model.

We also notice that the linear model has the merit of showing how the buckling resistance increases with the material performances of the cohesive zone. This is not as obvious in the case of the other two models.

Table 4. Delamination buckling simulation results

Source	Sum Sq.	d.f.	Mean Sq.	*F*	Prob>F
Qdc	1.07E+08	2	5.34E+07	10.02	2.77E-02
De	1.04E+08	2	5.22E+07	9.79	0.288
Error	2.13E+07	4	5.33E+06		
Total	2.33E+08	8			

Table 5. Delamination buckling simulation results

Source	Sum Sq.	d.f.	Mean Sq.	*F*	Prob>F
Qdc	1.07E+08	2	5.34E+07	Inf	NaN
De	1.04E+08	2	5.22E+07	Inf	NaN
Qdc*De	2.13E+07	4	5.33E+06	Inf	NaN
Error	−1.49E−07	0	0		
Total	2.33E+08	8			

5. CONCLUSION

In the present work, the problem of buckling in interaction or not with delamination occurring in a composite panel subjected to axial compression was simulated. The method of cohesive elements was used. We performed a parametric study to quantify the influence of parameters describing the cohesive behavior on buckling resistance in the presence of circular delamination. In the studied field of parameters, the results obtained showed a certain sensitivity with respect to the amplitude of the initial displacements out of planes associated with the imperfection. Buckling occurs more easily as the magnitude of the defect increases. We have also found that the two criteria of cohesive behavior play an important role. A significant increase in the maximum load is observed as the initiation threshold or the stiffness of the cohesive members increases. Further studies are needed to objectively quantify the delamination buckling interaction and in particular to analyze the influence of delamination geometry and its position on strength.

NOMENCLATURE

ABBREVIATIONS

BVID	Barely Visible Impact Damage
CFRP	carbon fiber reinforced polymer
CZM	Cohesive Zone Model
Df	degrees of freedom
F	F-statistic is the ratio of the mean squared errors
EDT	Energy Derivative Technique
FEM	Finite Element Method
LMR	linear mechanics of rupture
Mean Sq	Mean square of the error term
PEEK	Polyether-ether-ketone
Sum Sq	Sum of Squared Elements
VAT	Variable angle tow
VCCT	Virtual Crack Closure Technique

SYMBOLS

d	Global damage variable
D_{sr}	Constitutive operator
G	Energy release rate
G_I	Mode I energy release rate
G_{II}	Mode II energy release rate
G_{III}	Mode III energy release rate
G_C	Mixed-mode fracture toughness
G_{IC}	Mode I critical energy release rate
G_{IIC}	Mode II critical energy release rate
G_{IIIC}	Mode III critical energy release rate
$G_{cisaillement}$	Shear mode energy release rate
G_T	Total energy release rate
Kp	Penalty stiffness

N	Interlaminar tensile strength
S and T	Interlaminar shear forces
$\boldsymbol{\beta}$	Mix mode ratio
$\boldsymbol{\delta_3^f}$, $\boldsymbol{\delta_2^f}$, $\boldsymbol{\delta_1^f}$	Final separations relative to the crack propagation under single-mode loading
$\boldsymbol{\delta_m}$	Equivalent separation
$\boldsymbol{\tau_m}$	Corresponding equivalent traction
$\boldsymbol{\delta_m^f}$	Final equivalent separation associated to complete debonding
$\overline{\boldsymbol{\delta_{sr}}}$	Kronecker Delta

REFERENCES

[1] M. Chaves-Vargas, a. Dafnis, H. G. Reimerdes, and K. U. Schröder, "Modal parameter identification of a compression-loaded CFRP stiffened plate and correlation with its buckling behaviour," *Prog. Aerosp. Sci.*, vol. 78, pp. 39–49, 2015.

[2] E. S. Greenhalgh, "Delamination-dominated failures in polymer composites," *Fail. Anal. Fractography Polym. Compos.*, pp. 164–237, 2009.

[3] N. J. Pagano and G. A. Schoeppner, "Delamination of polymer matrix composites: problems and assessment," *Compr. Compos. Mater.*, pp. 433–528, 2000.

[4] I. Feddal, A. Khamlichi, and K. Ameziane, "Resistance to buckling of a stiffened panel under axial compression; Effect of imperfections resulting from welding process," *Proced. Manufacturing*, vol. 32, 2019.

[5] A. Shahrjerdi, and B. Bahramibabamiri, "The effect of different geometrical imperfection of buckling of composite cylindrical shells subjected to axial loading," *Int. J. Mech. Mater. Eng.*, vol. 10, no. 1, 2015.

[6] R. Degenhardt, K. Rohwer, D. Wilckens, and J. Tessmer, "Improved material exploitation of composite airframe structures by accurate simulation of collapse - the COCOMAT project," *Tech. Isr. Inst. Technol. - 48th Isr. Annu. Conf. Aerosp. Sci. 2008*, vol. 1, no. March, pp. 458–63, 2008.

[7] N. P., M. T. H. Ku, and H. Wang, *A Review on the Tensile Properties of Natural Fibre Reinforced Polymer Composites*. University of Southern Queensland, 2014.

[8] M. J. Pavier, and M. P. Clarke, "Experimental techniques for the investigation of the effects of impact damage on carbon-fibre composites," *Compos. Sci. Technol.*, vol. 55, no. 2, pp. 157–69, 1995.

[9] Z. Juhász and A. Szekrényes, "The effect of delamination on the critical buckling force of composite plates: experiment and simulation," *Compos. Struct.*, vol. 168, pp. 456–64, 2017.

[10] X. Chen, Z. Wu, G. Nie, and P. Weaver, "Buckling analysis of variable angle tow composite plates with a through-the-width or an embedded rectangular delamination," *Int. J. Sol. Struct.*, vol. 138, pp. 166–80, 2018.

[11] S. Mondal, and L. S. Ramachandra, "Nonlinear dynamic pulse buckling of imperfect laminated composite plate with delamination," *Int. J. Sol. Struct.*, vol. 198, pp. 170–82, 2020.

[12] A. A. Griffits, "The phenomena of rupture and flow in solids," *Masinovedenie*, no. 1, pp. 9–14, 1995.

[13] A. A. Griffith, "The Phenomena of Rupture and Flow in Solids VI . The Phenomena of Rupture and Flow in Solids . larger question of the nature of intermolecular cohesion . The original object of the work , which was carried out at the Royal Aircraft Estab- lishment, was t," *Philos. Trans. R. Soc. Lond. Ser. A, Contain. Pap. a Math. or Phys. Character*, vol. 221, no. 1921, pp. 163–98, 1921.

[14] D. Albiol, *Buckling Analyses of Composite Laminated Panels with Delamination*. Facolta di Ingegneria Industriale - Politecnico Di Milano, 2010.

[15] A. C. Orifici, R. S. Thomson, R. Degenhardt, C. Bisagni, and J. Bayandor, "Development of a degradation model for the collapse analysis of composite aerospace structures," *Proc. 3rd Eur. Conf. Comput. Mech. Solids, Struct. Coupled Probl. Eng.*, no. July, 2006.

[16] A. D. Dimarogonas, "Vibration of cracked structures: a state of the art review," *Eng. Fract. Mech.*, vol. 55, no. 5, pp. 831–57, 1996.

[17] D. S. Dugdale, "Yielding of steel sheets containing slits," *J. Mech. Phys. Sol.*, vol. 8, no. 2, pp. 100–4, 1960.

[18] P. P. Camanho, C. G. Davila, and S. S. Pinho, "Fracture analysis of composite co-cured structural joints using decohesion elements," *Fatigue Fract. Eng. Mater. Struct.*, vol. 27, no. 9, pp. 745–57, 2004.

[19] F. Marulo, M. Guida, L. Maio, and F. Ricci, "Numerical simulations and experimental experiences of impact on composite structures," in *Dynamic Response and Failure of Composite Materials and Structures*, V. Lopresto, L. Antionio, and A. Serge, Eds, Woodhead Publishing, 2017, pp. 85–125.

[20] M. R. Wisnom, Z. J. Petrossian, and M. I. Jones, "Interlaminar failure of unidirectional glass/epoxy due to combined through thickness shear and tension," *Compos. Part A. Appl. Sci. Manuf.*, vol. 27, no. 10, pp. 921–9, 1996.

[21] P. Camanho, and C. G. Davila, "Mixed-mode decohesion finite elements in for the simulation composite of delamination materials," *Nasa*, vols TM-2002-21, no. June, pp. 1–37, 2002.

[22] M. Kenane, and M. L. Benzeggagh, "Mixed-mode delamination fracture toughness of unidirectional glass/epoxy composites under fatigue loading," *Compos. Sci. Technol.*, vol. 57, no. 5, pp. 597–605, 1997.

[23] J. Edward, M. Wu, and R. C. Router, *Crack Extension in Fiberglass Reinforced Plastics*. Urbana, Illinois, 1965, Contract N° 64-0178-d.

[24] G. Marom, *Environmental Effects on Fracture Mechanical Properties of Polymer Composites*, vol. 6, no. C. Elsevier Science Publishers B.V., 1989.

[25] A. J. Brunner, B. R. K. Blackman, and P. Davies, "A status report on delamination resistance testing of polymer-matrix composites," *Eng. Fract. Mech.*, vol. 75, no. 9, pp. 2779–94, 2008.

[26] N. F. Knight, "User-defined material model for thermo- mechanical progressive failure analysis," no. December, 2008.

[27] T. Ceglar, "Finite element method simulations of the delamination in laminated composite structures," no. February, 2017.